TTC13 expression and STAT3 activation may form a positive feedback loop to promote ccRCC progression

Lingling Xie [Equal first author, 1], **Yu Fang** [Equal first author, 2], **Jianping Chen** [1], **Wei Meng** [3], **Yangbo Guan** [Corresp., 3], **Wenliang Gong** [Corresp. 2, 4]

[1] Department of Laboratory Medicine, Affiliated Hospital of Nantong University, Nantong, China

[2] Department of Urology, The First Affiliated Hospital of Naval Medical University (Shanghai Changhai Hospital), Shanghai, China

[3] Department of Urology, Affiliated Hospital of Nantong University, Nantong, China

[4] Department of Urology, The Third Affiliated Hospital of Naval Medical University (Shanghai Eastern Hepatobiliary Surgery Hospital), Shanghai, China

Corresponding Authors: Yangbo Guan, Wenliang Gong
Email address: guanyangbo123@163.com, gongwl_uro@163.com

Background: Renal cell carcinoma (RCC) originates from renal tubular epithelial cells and is mainly classified into three histological types, including clear cell renal cell carcinoma (ccRCC) which accounts for about 75% of all kidney cancers and is characterized by its strong invasiveness and poor prognosis. Hence, it is imperative to understand the mechanisms underlying the occurrence and progression of ccRCC to identify effective biomarkers for the early diagnosis and the prognosis prediction.

Methods: The mRNA level of TTC13 was quantified by RT-PCR, while the protein level was determined by western blot and immunohistochemistry (IHC) staining. Cell proliferation was measured by cck-8, and cell apoptosis was detected by flow cytometry. The binding of STAT3 to the promoter region of TTC13 was determined by the luciferase reporter assay and chip experiments. STAT3 nuclear translocation was assessed by immunofluorescence staining.

Results: We found that TTC13 was up-regulated in ccRCC, and TTC13 promoted cell proliferation as well as inhibited cell apoptosis and autophagy of ccRCC through wnt/β-catenin and IL6-JAK-STAT3 signaling pathways. Furthermore, TTC13 might play a role in the immune infiltration and immunotherapy of ccRCC. Mechanistically, STAT3 activated the transcription of TTC13 gene.

Conclusions: STAT3 directly regulated TTC13 expression through a positive feedback loop mechanism to promote ccRCC cell proliferation as well as reduce cell apoptosis and autophagy. These findings suggested new and effective therapeutic targets for more accurate and personalized treatment strategies.

TTC13 expression and STAT3 activation may form a positive feedback loop to promote ccRCC progression

Lingling Xie[1] ,Yu Fang[2] ,Jianping Chen[1],Wei Meng[3],Yangbo Guan[3] ,Wenliang Gong[2, 4]

[1]Department of Laboratory Medicine, Affiliated Hospital of Nantong University, Nantong, China

[2]Department of Urology, The First Affiliated Hospital of Naval Medical University (Shanghai Changhai Hospital), Shanghai, China

[3]Department of Urology, Affiliated Hospital of Nantong University, Nantong, China

[4]Department of Urology,The Third Affiliated Hospital of Naval Medical University (Shanghai Eastern Hepatobiliary Surgery Hospital), Shanghai, China

Correspondence to: Dr. Yangbo Guan and Dr. Wenliang Gong, Department of Urology, Affiliated Hospital of Nantong University, No.20 Xisi Road, Nantong 226001, China; Department of Urology, The Third Affiliated Hospital of Naval Medical University (Shanghai Eastern Hepatobiliary Surgery Hospital), Shanghai 200433, China. E-mail: guanyangbo123@163.com;gongwl_uro@163.com.

Abstract

Background: Renal cell carcinoma (RCC) originates from renal tubular epithelial cells and is mainly classified into three histological types, including clear cell renal cell carcinoma (ccRCC) which accounts for about 75% of all kidney cancers and is characterized by its strong invasiveness and poor prognosis. Hence, it is imperative to understand the mechanisms underlying the occurrence and progression of ccRCC to identify effective biomarkers for the early diagnosis and the prognosis prediction.

Methods: The mRNA level of TTC13 was quantified by RT-PCR, while the protein level was determined by western blot and immunohistochemistry (IHC) staining. Cell proliferation was measured by cck-8, and cell apoptosis was detected by flow cytometry. The binding of STAT3 to the promoter region of TTC13 was determined by the luciferase reporter assay and chip experiments. STAT3 nuclear translocation was assessed by immunofluorescence staining.

Results: We found that TTC13 was up-regulated in ccRCC, and TTC13 promoted cell proliferation as well as inhibited cell apoptosis and autophagy of ccRCC through wnt/β-catenin and IL6-JAK-STAT3 signaling pathways. Furthermore, TTC13 might play a role in the immune infiltration and immunotherapy of ccRCC. Mechanistically, STAT3 activated the transcription of TTC13 gene.

Conclusions: STAT3 directly regulated TTC13 expression through a positive feedback loop mechanism to promote ccRCC cell proliferation as well as reduce cell apoptosis and autophagy. These findings suggested new and effective therapeutic targets for more accurate and personalized treatment strategies.

Keywords: TTC13, Clear cell renal cell carcinoma, Biomarker, Immunity, Prognosis, cell autophagy

Introduction

Renal cell carcinoma (RCC) ranks as the seventh most frequently diagnosed cancer and the second most prevalent urinary system-related cancer worldwide. The incidence of RCC varies among different regions with the highest incidence in developed countries. RCC mainly includes three types, among which clear cell renal cell carcinoma (ccRCC) has the highest mortality rate (Piao et al. 2023). ccRCC is characterized by hematuria, pain, and lump in the kidney area mostly detected in its later stage, accounting for about 75% of all kidney cancers; nevertheless, ccRCC is often asymptomatic or insidious at its early stage. Although the diagnosis and the clinical treatment of ccRCC have been significantly improved during recent years, the prognosis of patients with advanced ccRCC is still suboptimal owing to the high risk of metastasis and poor response to radiotherapy and chemotherapy (Kase et al. 2023). Therefore, understanding the mechanisms underlying the occurrence and progression of ccRCC is critical for the identification of biomarkers for early diagnosis, treatment selection, and prognosis prediction.

Tetratricopeptide repeat domain 13 (TTC13) is a member of the large tetratricopeptide repeats (TPR) family of proteins which consists of a degenerate, 34 amino acid repeats, and is expressed in 27 human tissues including the brain, bladder, heart, and lung. TPR-containing proteins are found not only in many organisms but also in various subcellular locations, such as cytoplasm, nucleus, and mitochondria. Functionally, the TPR domain plays a part in cell cycle, transcription and protein transport (Leontiou et al. 2019). Although the role of TPR-related proteins in tumors has been reported in leukemia, liver cancer, and gastric cancer (El-Daher et al. 2018; Shaheen et al. 2020), the function of TTC13 in tumors is not clear, and the expression and biological functions of TTC13 in ccRCC need to be determined.

In this study, we performed multiple bioinformatics analyses and validation experiments to explore the expression, biological functions, and prognostic value of TTC13 in ccRCC. We for the first time found that TTC13 was upregulated in ccRCC, and TTC13 expression was associated with several pathological features. Particularly, TTC13 could modulate immune infiltration and immunotherapy. Our findings suggested that TTC13 may act as a valuable independent predictive biomarker for the diagnosis of ccRCC. Our mechanistic studies indicated that TTC13 might contribute to ccRCC progression via regulating Wnt/β-catenin and IL6-JAK-STAT3 signal pathways. Taken together, TTC13 may play a critical role in ccRCC occurrence and progression, and TTC13 signaling axis may serve as new and effective therapeutic targets for the exploration

of more accurate and personalized treatment strategies.

Materials and methods

Bioinformatics analysis

TTC13 expression data as well as the corresponding clinical data were obtained from The Cancer Genome Atlas (TCGA) database. The raw data were pre-processed using either log2 transformation or normalization and then were analyzed using R software v4.1.3. Differential gene expression of TTC13 was calculated using the "limma" R package (Wang et al. 2020), with a cut-off criterium of |log2 fold change (FC)| > 1 and a false discovery rate (FDR) < 0.05.

Human ccRCC tissue samples and cell lines

The tumor and adjacent non-cancerous tissues were obtained from the Affiliated Hospital of Nantong University. This study was approved by the hospital's ethics committee (Institutional Review Board approval number: 2022-K003-02), and all patients offered written informed consents for the use of their samples. Normal HK-2 cell line and three ccRCC cell lines: A498, 786-0 and Caki-1 were obtained from either the Cell Bank of Chinese Academy of Sciences (Shanghai, China) or Procell Life Science & Technology Co. Ltd. (Wuhan, China). All cell lines were cultured according to the required culture conditions.

Antibodies

We used the following antibodies: TTC13(AP13674a,abcepta,1:1000), Bax(ab32503, abcam,1:1000), Bcl-2(ab182858,abcam,1:1000), IL-6(12912,CST,1:1000), cleaved-caspase-3(9664, CST, 1:1000), LC3Ⅱ/Ⅰ (ab192890, abcam, 1:1000), P62(88588, CST, 1:1000),JAK2(ab108596, abcam, 1:1000), Ki67(ab92742, abcam, 1:1000), MMP9(13667, CST, 1:1000), phosphor-JAK2(ab32101, abcam, 1:1000), phosphor-STAT3(ab76315, abcam, 1:1000), STAT3(ab68153, abcam, 1:1000), β-catenin(ab32572, abcam, 1:1000), GAPDH (5174, CST, 1:1000)and β-actin(ab8226, abcam, 1:1000).

Quantitative Real-Time Polymerase Chain Reaction (qRT-PCR)

qRT-PCR was carried out to examine the expression level of TTC13 in 64 paired ccRCC tumor and adjacent non-cancerous samples using ABI 7500. Experiments were performed in duplicate, and the thresholdcycle (CT) values were averaged. TTC13 gene expression was normalized to GAPDH expression resulting in the ΔCT value, where ΔCt = Ct Target − Ct GAPDH. The relative expression level was determined

by $2^{-\Delta CT}$as previously described (Aguilar-Briseno et al. 2020).The primers were synthesized by Tsingke Biotech (Shanghai, China), and the primer sequences were denoted as follows: for TTC13, forward 5′-GACTCAGACTGCGAACCCAA-3′ and reverse 5′- ACTTGGCCTGGCTCAGAATC-3′; for GAPDH, the forward primer sequence was 5′-GAGTCAACGGATTTGGTCGT-3′ and the reverse primer sequence was 5′-GACAAGCTTCCCGTTCTCAG-3′.

Cell transfection

shRNA for TTC13 gene silencing and the plasmid for TTC13 overexpression were purchased from GenePharma (Shanghai, China). Two shRNAs were used to exclude off-target effects: shRNA1 (5′-GCAGTGAATGACCTCACTAAA-3′) and shRNA2(5′-GCTTACAGGAAGCCCTTAAGA-3′). The TTC13 shRNAs or TTC13 overexpression plasmid was transfected into ccRCC cells using the Lipofectamine 3000 reagent (L3000075, Invitrogen), and transfection efficiency was confirmed by western blot analysis. Cells were collected for in vitro functional experiments 48 h after transfection. Stable TTC13 knockdown of 786-0 cells was obtained by shRNA lentivirus infection and further puromycin selection(Tandon Net al. 2018). shRNA for STAT3 gene silencing and the plasmid for STAT3 overexpression were also purchased from GenePharma (Shanghai, China).

Cell proliferation and apoptosis

Cell proliferation was determined by a CCK-8 detection kit (C0038, Beyotime, Haimen, China). Briefly, transfected cells were seeded into 96-well plate (5,000/well) and cultured for the indicated times. CCK-8 solution (10 μl) was added to each well at specific time points, and the absorbance at 450 nm was determined by a plate reader. Each experiment was independently repeated for three or five times. For apoptosis assay, the ccRCC cells were collected, stained with the annexin V-conjugated fluorescein isothiocyanate (FITC) and the propidium iodide (PI) (C1062S-2, Beyotime, Haimen, China) following the manufacturer's instructions, and analyzed using FACScan^{TM} flow cytometer (BD Biosciences).

Mouse tumor xenografts

Six-week-old male null mice (weighted about 18g) were obtained from Jihui Laboratory Animal Care Co., Ltd. (Shanghai, China) and were randomly separated into two groups for subcutaneous injection with 786-0 cells (2×10^6/200μl PBS) either stably expressing NC empty vectoror TTC13 shRNA. The xenograft tumor

136 growth was monitored every 5 days, and at day 35, the tumors were dissected, weighed, and subjected to
137 immunohistochemistry (IHC) staining. All experimental procedures were performed in accordance with the
138 institutional guidelines approved by the Shanghai Changhai Hospital, Naval Medical University.

139 **Western blot analysis**

140 Total proteins were extracted from ccRCC cells using the protein extraction kit (P0013B, Beyotime,
141 Haimen, China) and quantified by the NanoPhotometer (Implen, Inc., CA, USA). Then, the proteins were
142 separated by the SDS-PAGE and transferred onto the PVDF membranes, followed by incubation with the
143 corresponding primary antibodies. After extensive washing, the PVDF membranes were incubated with the
144 secondary antibodies, and the specific protein bands were visualized by using an enhanced chemiluminescence
145 (ECL) kit (P0018M, Beyotime, Haimen, China) and imaged in a gel imaging system.

146 **Immunohistochemistry (IHC) staining**

147 The protein expression and distribution of β-catenin, Ki67, MMP9, phospho-STAT3, cleaved caspase-3
148 and TTC13 were examined by IHC of paraffin-embedded sections of ccRCC and adjacent non-cancerous
149 tissues. Briefly, after deparaffinization and rehydration, the paraffin slides were treated with citric acid buffer
150 solution (pH=6.0) at 121 °C for 15 minutes, followed by treatment with 3% hydrogen peroxide for 20 min.
151 Slides were blocked with 1% BSA for 15 minutes and then incubated with primary antibody (1:50 dilution) at
152 4 °C overnight. After extensive washing, the slides were incubated with goat anti-rabbit IgG-HRP secondary
153 antibody (1:100 dilution) at room temperature for 1 h and then counterstained with hematoxylin for 30 s.
154 Lastly, the conventional dehydration was performed, and the slides were examined as well as imaged under a
155 microscope (DM500, Leica).

156 **Immunofluorescence (IF) staining**

157 Standard IF staining procedure was employed. Briefly, cells were seeded onto coverslips, fixed with 4%
158 paraformaldehyde, permeabilized with 0.1% Triton, and then incubated with the primary antibodies at 4 °C
159 overnight followed by incubation with the secondary antibodies for 1 h. The cells were subsequently stained
160 with 0.1 μg/ml DAPI for 1 minute at room temperature in the dark. The coverslips were mounted, and the
161 images were acquired using a fluorescence microscope.

162 **Luciferase reporter assay and Chromatin immunoprecipitation (ChIP) assay**

For luciferase reporter assay, Caki-1 cells treated with AG490 were transiently co-transfected with pGL3-basic-TTC13 reporter plasmid and pRL-TK expression construct using Lipofectamine 3000 reagent according to the manufacturer's instructions. At 48h after transfection, the cells were harvested, and the luciferase activity was quantified using the Bright-Glo™ Luciferase assay kit (E1910, Promega Corporation), which was normalized to the Renilla luciferase activity. Each experiment was performed in triplicate. For the Chip assay, a standard Chip assay protocol was used for cells crosslinking, nuclear isolation, and chromatin fragmentation. The fragmented chromatin was incubated with anti-STAT3 antibody at 4°C overnight, and the eluted chromatin was subjected to quantitative PCR analysis. IgG was used as a negative control.

Statistical analysis

Statistical analyses were conducted using GraphPad Prism 8.0 and SPSS Statistics 22.0. Data were presented as median and standard error of the mean (SEM). To compare the overall survival between two groups, Kaplan-Meier (K-M) curves and the log-rank test were employed. Paired cases were carried out by using t-test, while the prognostic value of TTC13 was evaluated using the univariate and multivariate Cox regression analyses. A P-value<0.05 was regarded as statistically significant.

Results

TTC13 was upregulated in ccRCC

As shown in Figure 1A, the expression level of TTC13 was different between various tumors and normal tissues with a significant upregulation in ccRCC (Figure 1B) ($P< 0.001$), which was supported by the data from the paired tumor and non-cancerous samples (Figure 1C). Consistently, qRT-PCR analysis (tumor=64, normal=64) showed that the mRNA level of TTC13 was significantly higher in ccRCC tissues than in normal tissues ($P<0.001$) (Figure 1D) which was further confirmed by western blotting (Figure 1E, G) and IHC (Figure 1F). Furthermore, the ROC curves were used to evaluate the efficacy of TTC13 expression for ccRCC diagnostic prediction, suggesting that TTC13 level could serve as a diagnostic biomarker (Figure 1H). Moreover, the ccRCC patients were divided into low- and high-expression groups based on the median expression value of TTC13, and the K–M survival curve analysis showed that the overall survival of the high-expression group was worse than that in the low-expression group ($P< 0.001$) (Figure 1I), indicating the negative association between TTC13 level and patient overall survival.

TTC13 promoted the proliferation and inhibited the apoptosis and autophagy of ccRCC cells

We next explored the biological functions of TTC13 in ccRCC. CCK-8 assay revealed that knockdown of TTC13 inhibited the proliferation of HK-2,786-0 and Caki-1 cells (Figure 2A). On the other hand, the flow cytometry analysis revealed that knockdown of TTC13 increased the apoptosis of HK-2 and ccRCC cells (Figure 2B). In support with these findings, western blotting results suggested that the levels of p62 and BCL-2 protein in shTTC13 transfected HK-2, 786-0 and Caki-1 cells were significantly decreased, while the levels of Bax and cleaved caspase-3 as well as the ratio of LC3-II/I was significantly increased. Conversely, TTC13 overexpression resulted in the opposite effects (Figure 2C), suggesting that TTC13 was involved in the regulation of renal cancer cell survival and autophagy.

TTC13 silencing inhibited tumor growth in vivo

To explore the effect of TTC13 on tumor growth in vivo, we subcutaneously injected 786-0 cells transfected with either TTC13 NC or shRNA plasmid into nude mice and found that the tumor volume and weight of the shRNA group were evidently smaller than that of the NC group (Figure 3A, B, C, D). Moreover, IHC staining showed that the expression of TTC13, Ki67, MMP9, β-catenin and p-STAT3 were lower while cleaved caspase 3 was higher in the shRNA group than in the NC group (Figure 3E), which was further validated by western blot analysis (Figure 3F). Together, these results indicated that knockdown of TTC13 effectively inhibited tumor growth in vivo.

Analysis of TTC13-related signaling pathways in ccRCC

To understand the role of TTC13 in the pathogenesis of ccRCC, GSVA analysis was performed by using TTC13-high or -low expression datasets to explore the TTC13-regulated signaling pathways. We identified TTC13 associated up- and down-regulated signaling pathways, including Wnt/β-catenin, IL6-JAK-STAT3, interferon-alpha, interferon-gamma, E2F targets signaling pathways (Figure 4A), suggesting that TTC13 expression may be related to cellular immunity and cell cycle regulation. To validate the findings from bioinformatics analysis, we focused our in vitro experiments on two signaling pathways that have been well known to be involved in tumorigenesis. Specifically, we experimentally determined whether Wnt/β-catenin and IL6-JAK-STAT3 signal pathways were activated in ccRCC by examining the expression of TTC13, β-catenin, JAK2, p-STAT3, STAT3 and p-JAK2 in ccRCC tumor tissues as well as the adjacent normal tissues.

Western blotting results demonstrated an activated Wnt/β-catenin and IL6-JAK-STAT3 signal pathways in ccRCC (Figure 4B, C). To directly demonstrate the relationship between TTC13 and Wnt/β-catenin and IL6-JAK-STAT3 signal pathways, we assessed the effects of TTC13 overexpression or knockdown on these two signaling activities. We found that overexpression of TTC13 enhanced, while TTC13 knockdown inhibited, the expression of β-catenin, p-JAK-2 and p-STAT3 in ccRCC cells, suggesting the regulation of TTC13 in Wnt/β-catenin and IL6-JAK-STAT3 pathways (Figure 4D).

TTC13 contributed to ccRCC progression via Wnt/β-catenin and IL6-JAK-STAT3 signal pathways

Having demonstrated that TTC13 activated Wnt/β-catenin and IL6-JAK-STAT3 signal pathways in ccRCC, we speculated that TTC13 might contribute to ccRCC progression through the above two signaling pathways. To test this hypothesis, we performed rescued experiments using a specific inhibitor of Wnt/β-catenin ICG001 or IL6-JAK-STAT3 signaling pathway AG490 and found that the inhibitors could attenuate the growth-promoting effect of TTC13(Figure 5A,C). Western blot analysis showed the similar results (Figure 5D). Furthermore, we determined the dose response curve of cells to a 3-day inhibitor treatment and revealed that TTC13 overexpression increased the IC50 of AG490 and ICG001, indicating that TTC13 enabled ccRCC cells to resistant to drug treatment (Figure 5B). Taken together, the above results demonstrated that TTC13 promoted ccRCC progression at least partly through activating Wnt/β-catenin and IL6-JAK-STAT3 signal pathways.

STAT3 activated the transcription of TTC13 gene

More importantly, we investigated the molecular mechanisms underlying the elevated TTC13 expression in ccRCC. Since we observed that TTC13 could activate the IL6-JAK-STAT3 signaling pathway, we postulated that STAT3 might enter the nucleus upon TTC13 overexpression. Indeed, immunofluorescence staining confirmed a significant translocation of STAT3 from cytoplasm to nucleus when TTC13 was overexpressed (Figure 6D). Since STAT3 is a transcription factor, we next explored whether STAT3 affected the activity of the TTC13 promoter. In line with this notion, transcription factor binding profile database JASPAR has identified several potential STAT3 binding sites on TTC13 promoter (http://jaspar.genereg.net/) (Figure 6A, B). Consistently, TTC13 expression was decreased by STAT3 knockdown while TTC13 expression was increased by STAT3 overexpression (Figure 6C). To further demonstrate the transcriptional

regulation of TTC13 by STAT3, we carried out the luciferase reporter assay and found that the TTC13 promoter-driven luciferase activity in AG490-treated Caki-1 cells were significantly reduced (Figure 6F). Chip assay further confirmed that STAT3 directly bound to the TTC13 promoter (Figure 6E), suggesting that STAT3 might directly regulated TTC13 expression through a positive feedback loop mechanism to promote ccRCC cell proliferation, as well as to reduce cell apoptosis and autophagy.

Discussion

ccRCC is the most prevalent histological subtype, accounting for more than 75% of all diagnosed kidney tumors, and has the characteristics of strong invasiveness and poor prognosis (Narisawa et al. 2023; Ye et al. 2023). Tetratricopeptide repeat domain 13 (TTC13) is a member of a large family of proteins named tetratricopeptide repeats (TPR), which contains more than 5,000 members. So far, to the best of our knowledge, there is no report on the expression and functions of TTC13 in ccRCC. In this study, we analyzed the expression level and the prognostic value of TTC13 in ccRCC as well as explored its biological functions via both the bioinformatics analysis (Figure1s-5s) and the experimental confirmation. Our experimental results showed an upregulation of TTC13 at both mRNA and protein levels in ccRCC cells as well as in ccRCC tissues. In addition, ccRCC patients with high TTC13 expression had poor prognosis. Furthermore, overexpression of TTC13 promoted the proliferation of ccRCC cells, while inhibited the apoptosis and autophagy of cells. Hence, our results suggested that TTC13 might play a key role in the occurrence and progression of ccRCC (Figure 7).

Accumulating evidence has revealed that the dysregulation of the Wnt/β-catenin signal pathway contributes to the development and progression of several solid tumors and hematological malignancies (Di Bartolomeo et al. 2023; Han et al. 2023; Li et al. 2022; Muto et al. 2023). In this study, we discovered that the Wnt/β-catenin signal pathway was also abnormally expressed in ccRCC, suggesting the involvement of Wnt/β-catenin in ccRCC. In addition, IL6-JAK-STAT3 pathway is abnormally overactivated in numerous cancer types, which is often associated with poor outcomes (Ni et al. 2020; Siersbaek et al. 2020; Zhan et al. 2021). In this study, we found that the IL6-JAK-STAT3 signal pathway was activated in ccRCC, suggesting the therapeutic significance of this pathway. In support with our findings, Zhan et al. also identified the IL6-JAK-STAT3 signal as a potential risk factor in ccRCC by univariate and multivariate Cox regression analysis (Zhan

et al. 2021).

Our subsequent study demonstrated that overexpression of TTC13 could activate the IL6-JAK-STAT3 and Wnt/β-catenin signal pathways, whereas knockdown of TTC13 suppressed these two signaling pathways. Further experiments revealed that TTC13 promoted ccRCC cell proliferation and restrained apoptosis or autophagy through IL6-JAK-STAT3 and Wnt/β-catenin signal pathways. Consistent with our findings, Wang et al. (Wang et al. 2021) had reported that CENPA promoted the progression of ccRCC by activating the Wnt/β-catenin signal pathway. In addition, a recent study had revealed the Wnt/β-catenin signal-induced ARL4C expression in ccRCC (Zhang et al. 2022). On the other hand, several studies had indicated that some genes acted as tumor suppressors by inhibiting the Wnt/β-catenin signal pathway in ccRCC. For example, Gorkaet al. (Gorka et al. 2021) had reported that β-catenin in ccRCC cells was significantly reduced at both mRNA and protein levels by MCPIP1 overexpression. In line with these findings, Xu et al. (Xu et al. 2022) demonstrated that the upregulation of SDHA resulted in a significant suppression of the Wnt/β-catenin signal pathway by decreasing the β-catenin expression in ccRCC. Moreover, the activator of Wnt/β-catenin signal pathway can attenuate the inhibition on the malignancy of ccRCC cells caused by TLN2 overexpression (Cai et al. 2022). And SOX17 displayed the similar function as TLN2(Wang et al. 2021a). These results, together with our findings, provide supporting evidence that Wnt/β-catenin signaling pathway is a crucial regulator in the progression of ccRCC, highlighting the clinical significance of targeting this signaling pathway. As for IL6-JAK-STAT3 signaling pathway, consistent with our findings, wang et al. (Wang et al. 2018) also reported that IL-6 and p-STAT3 expressions in renal cell carcinoma tissues was obviously higher compared with adjacent normal tissues. Another study found that knockdown of circ_0000274 RNA expression significantly reduced the protein levels of p-JAK1/JAK1 and p-STAT3/STAT3 in 786-0 and A498 cells, while inhibiting miR-338-3p expression reversed this effect (Qi et al. 2022). In addition, the conditioned medium of TAMs increased the phosphorylation level of STAT3 in RCC cells (Chen et al. 2022). Furthermore, it has been reported that tumor-associated macrophages promote RCC epithelial-mesenchymal transition, migration, and invasion via activating IL-6/STAT3 signaling. Consistent with these findings, another study showed that the total pSTAT3 and nuclear pSTAT3 levels were prominently increased in ccRCC tissues compared with the adjacent tissues (Song et al. 2019). Chae et al. (Chae et al. 2020) also reported that Thymoquinone effectively

prevented the phosphorylated form of STAT3 from entering the nucleus and binding to DNA to activate the transcription of target genes. Similarly, SIRT1 destabilized STAT3 through the ubiquitin-proteasome pathway, resulting in a decreased STAT3-dependent FGB expression, which in turn inhibited RCC cell proliferation (Chen et al. 2019). Collectively, these findings indicated that TTC13 may be associated with suppressed antitumor immune responses in the tumor microenvironment of ccRCC. Therefore, therapies targeting TTC13 as well as IL6-JAK-STAT3 signaling pathway may benefit ccRCC patients by simultaneously suppressing tumor cell growth and stimulating anti-tumor immunity.

One important finding of our study was that STAT3 bound to the promoter of TTC13 gene to upregulate the expression of TTC13, which in turn further activated the JAK2/STAT3 signal pathway to increase the nuclear import of STAT3, thereby forming a positive feedback loop to promote the progression of ccRCC. A recent investigation had also revealed that the JAK/STAT3 signaling pathway regulated RCC cell apoptosis and glycolysis through RNF7, as STAT3 directly binded to RNF7 promoter (Xiao et al. 2022). Taken together, these data suggested that IL6-JAK-STAT3 signal pathway played a significant role in the pathogenesis of ccRCC, providing the rationale of targeting this pathway in ccRCC treatment.

Nonetheless, this study also had some limitations. First, we used retrospective data from public databases, which needs further validation in larger cohorts of ccRCC patients with well-defined clinical staging and sufficient clinical data. In addition, the biological function of TTC13 in ccRCC need to be further investigated. Lastly, it is necessary to improve and standardize the detection method of TTC13 gene to increase the feasibility of clinical application.

Conclusions

In conclusion, we were the first to use a variety of bioinformatics methods and verification experiments to explore the expression and clinical value of TTC13 in ccRCC. Our results indicated that TTC13 may play a role in the proliferation, apoptosis, and autophagy of ccRCC. In addition, TTC13 may serve as a novel biomarker for the diagnosis and prognosis prediction for patients with ccRCC.

Funding This study was funded by Nantong Commission of Health (QN2022016).

Compliance with Ethical Standards Ethics statements

The study was approved and consented by the Ethics Committee of the Affiliated Hospital of Nantong University (2022-K003-02) and Naval Medical University, SYXK (Shanghai) 2022-0011. All patients provided written informed consent for the use of their tissue samples.

Conflict of Interest The authors declare that there is no conflict of interest.

Acknowledgments

We sincerely thank The Cancer Genome Atlas (TCGA) database for providing and managing patient data. The authors express their appreciation for the assistance by Dr Shaoqing Ju and Shanghai Changhai Hospital, Naval Medical University, which was instrumental in facilitating this research.

References

Aguilar-Briseno JA, Upasani V, Ellen BMT, Moser J, Pauzuolis M, Ruiz-Silva M, Heng S, Laurent D, Choeung R, Dussart P, Cantaert T, Smit JM, and Rodenhuis-Zybert IA. 2020. TLR2 on blood monocytes senses dengue virus infection and its expression correlates with disease pathogenesis. *Nat Commun* 11:3177. 10.1038/s41467-020-16849-7.

Cai J, Huang Z, Zhou J, Wu W, and Ye Y. 2022. TLN2 functions as a tumor suppressor in clear cell renal cell carcinoma via inactivation of the Wnt/beta-catenin signaling pathway.*Transl Androl Urol* 11:39-52. 10.21037/tau-21-914.

Chae IG, Song NY, Kim DH, Lee MY, Park JM, and Chun KS. 2020. Thymoquinone induces apoptosis of human renal carcinoma Caki-1 cells by inhibiting JAK2/STAT3 through pro-oxidant effect. *Food Chem Toxicol* 139:111253. 10.1016/j.fct.2020.111253.

Chen S, Qian S, Zhang L, Pan X, Qu F, Yu Y, Gu Z, Cui X, and Shen H. 2022. Tumor-associated macrophages promote migration and invasion via modulating IL-6/STAT3 signaling in renal cell carcinoma. *Int Immunopharmacol* 111:109139. 10.1016/j.intimp.2022.109139.

Chen Y, Zhu Y, Sheng Y, Xiao J, Xiao Y, Cheng N, Chai Y, Wu X, Zhang S, and Xiang T. 2019. SIRT1 downregulated FGB expression to inhibit RCC tumorigenesis by destabilizing STAT3. *Exp Cell Res* 382:111466. 10.1016/j.yexcr.2019.06.011.

Di Bartolomeo L, Vaccaro F, Irrera N, Borgia F, Li Pomi F, Squadrito F, and Vaccaro M. 2023. Wnt Signaling Pathways: From Inflammation to Non-Melanoma Skin Cancers. *Int J Mol Sci* 24. 10.3390/ijms24021575.

El-Daher MT, Cagnard N, Gil M, Da Cruz MC, Leveau C, Sepulveda F, Zarhrate M, Tores F, Legoix P, Baulande S, de Villartay JP, Almouzni G, Quivy JP, Fischer A, and de Saint Basile G. 2018. Tetratricopeptide repeat domain 7A is a nuclear factor that modulates transcription and chromatin structure. *Cell Discov* 4:61. 10.1038/s41421-018-0061-y.

Gorka J, Marona P, Kwapisz O, Waligorska A, Pospiech E, Dobrucki JW, Rys J, Jura J, and Miekus K. 2021.

MCPIP1 inhibits Wnt/beta-catenin signaling pathway activity and modulates epithelial-mesenchymal transition during clear cell renal cell carcinoma progression by targeting miRNAs. *Oncogene* 40:6720-6735. 10.1038/s41388-021-02062-3.

Han S, Jin X, Hu T, and Chi F. 2023. LAPTM5 regulated by FOXP3 promotes the malignant phenotypes of breast cancer through activating the Wnt/beta-catenin pathway. *Oncol Rep* 49. 10.3892/or.2023.8497.

Kase AM, George DJ, and Ramalingam S. 2023. Clear Cell Renal Cell Carcinoma: From Biology to Treatment. *Cancers (Basel)* 15. 10.3390/cancers15030665.

Leontiou I, London N, May KM, Ma Y, Grzesiak L, Medina-Pritchard B, Amin P, Jeyaprakash AA, Biggins S, and Hardwick KG. 2019. The Bub1-TPR Domain Interacts Directly with Mad3 to Generate Robust Spindle Checkpoint Arrest. *Curr Biol* 29:2407-2414 e2407. 10.1016/j.cub.2019.06.011.

Li R, Ke M, Qi M, Han Z, Cao Y, Deng Z, Qian J, Yang Y, and Gu C. 2022. G6PD promotes cell proliferation and dexamethasone resistance in multiple myeloma via increasing anti-oxidant production and activating Wnt/beta-catenin pathway. *Exp Hematol Oncol* 11:77. 10.1186/s40164-022-00326-6.

Muto S, Enta A, Maruya Y, Inomata S, Yamaguchi H, Mine H, Takagi H, Ozaki Y, Watanabe M, Inoue T, Yamaura T, Fukuhara M, Okabe N, Matsumura Y, Hasegawa T, Osugi J, Hoshino M, Higuchi M, Shio Y, Hamada K, and Suzuki H. 2023. Wnt/beta-Catenin Signaling and Resistance to Immune Checkpoint Inhibitors: From Non-Small-Cell Lung Cancer to Other Cancers. *Biomedicines* 11. 10.3390/biomedicines11010190.

Narisawa T, Naito S, Ito H, Ichiyanagi O, Sakurai T, Kato T, and Tsuchiya N. 2023. Fibroblast growth factor receptor type 4 as a potential therapeutic target in clear cell renal cell carcinoma. *BMC Cancer* 23:170. 10.1186/s12885-023-10638-3.

Ni JS, Zheng H, Ou YL, Tao YP, Wang ZG, Song LH, Yan HL, and Zhou WP. 2020. miR-515-5p suppresses HCC migration and invasion via targeting IL6/JAK/STAT3 pathway. *Surg Oncol* 34:113-120. 10.1016/j.suronc.2020.03.003.

Piao XM, Byun YJ, Zheng CM, Song SJ, Kang HW, Kim WT, and Yun SJ. 2023. A New Treatment Landscape for RCC: Association of the Human Microbiome with Improved Outcomes in RCC. *Cancers (Basel)* 15. 10.3390/cancers15030935.

Qi Q, Sun Y, Yang Y, and Liu Y. 2022. Circ_0000274 contributes to renal cell carcinoma progression by regulating miR-338-3p/NUCB2 axis and JAK1/STAT3 pathway. *Transpl Immunol* 74:101626. 10.1016/j.trim.2022.101626.

Shaheen R, Alsahli S, Ewida N, Alzahrani F, Shamseldin HE, Patel N, Al Qahtani A, Alhebbi H, Alhashem A, Al-Sheddi T, Alomar R, Alobeid E, Abouelhoda M, Monies D, Al-Hussaini A, Alzouman MA, Shagrani M, Faqeih E, and Alkuraya FS. 2020. Biallelic Mutations in Tetratricopeptide Repeat Domain 26 (Intraflagellar Transport 56) Cause Severe Biliary Ciliopathy in Humans. *Hepatology* 71:2067-2079. 10.1002/hep.30982.

Siersbaek R, Scabia V, Nagarajan S, Chernukhin I, Papachristou EK, Broome R, Johnston SJ, Joosten SEP, Green AR, Kumar S, Jones J, Omarjee S, Alvarez-Fernandez R, Glont S, Aitken SJ, Kishore K, Cheeseman D, Rakha EA, D'Santos C, Zwart W, Russell A, Brisken C, and Carroll JS. 2020. IL6/STAT3 Signaling Hijacks Estrogen Receptor alpha Enhancers to Drive Breast Cancer Metastasis. *Cancer Cell* 38:412-423 e419. 10.1016/j.ccell.2020.06.007.

Song J, Xu S, Zhang ZH, Chen YH, Gao L, Xie DD, Sun GP, Yu DX, and Xu DX. 2019. The correlation

between low vitamin D status and renal interleukin-6/STAT3 hyper-activation in patients with clear cell renal cell carcinoma. *Steroids* 150:108445. 10.1016/j.steroids.2019.108445.

Tandon N, Thakkar KN, LaGory EL, Liu Y, and Giaccia AJ. 2018. Generation of Stable Expression Mammalian Cell Lines Using Lentivirus. *Bio Protoc* 8. 10.21769/BioProtoc.3073.

Wang L, Wang Z, Zhu Y, Tan S, Chen X, and Yang X. 2021a. SOX17 Antagonizes the WNT Signaling Pathway and is Epigenetically Inactivated in Clear-Cell Renal Cell Carcinoma. *Onco Targets Ther* 14:3383-3394. 10.2147/OTT.S294164.

Wang Q, Xu J, Xiong Z, Xu T, Liu J, Liu Y, Chen J, Shi J, Shou Y, Yue C, Liu D, Liang H, Yang H, Yang X, and Zhang X. 2021b. CENPA promotes clear cell renal cell carcinoma progression and metastasis via Wnt/beta-catenin signaling pathway. *J Transl Med* 19:417. 10.1186/s12967-021-03087-8.

Wang Y, Fu D, Chen Y, Su J, Wang Y, Li X, Zhai W, Niu Y, Yue D, and Geng H. 2018. G3BP1 promotes tumor progression and metastasis through IL-6/G3BP1/STAT3 signaling axis in renal cell carcinomas. *Cell Death Dis* 9:501. 10.1038/s41419-018-0504-2.

Wang Z, Tang W, Yuan J, Qiang B, Han W, and Peng X. 2020. Integrated Analysis of RNA-Binding Proteins in Glioma. *Cancers (Basel)* 12. 10.3390/cancers12040892.

Xiao C, Zhang W, Hua M, Chen H, Yang B, Wang Y, and Yang Q. 2022. RNF7 inhibits apoptosis and sunitinib sensitivity and promotes glycolysis in renal cell carcinoma via the SOCS1/JAK/STAT3 feedback loop. *Cell Mol Biol Lett* 27:36. 10.1186/s11658-022-00337-5.

Xu X, Zhang N, Gao R, Wang J, Dai Z, and Bi J. 2022. Upregulation of SDHA inhibited proliferation, migration, and invasion of clear cell renal cell carcinoma cells via inactivation of the Wnt/beta-catenin pathway. *J Recept Signal Transduct Res* 42:180-188. 10.1080/10799893.2021.1883060.

Ye S, Li S, Qin L, Zheng W, Liu B, Li X, Ren Z, Zhao H, Hu X, Ye N, and Li G. 2023. GBP2 promotes clear cell renal cell carcinoma progression through immune infiltration and regulation of PD-L1 expression via STAT1 signaling. *Oncol Rep* 49. 10.3892/or.2023.8486.

Zhan C, Xu C, Chen J, Shen C, Li J, Wang Z, Ying X, Luo Z, Ren Y, Wu G, Zhang H, and Qian M. 2021. Development and Validation of an IL6/JAK/STAT3-Related Gene Signature to Predict Overall Survival in Clear Cell Renal Cell Carcinoma. *Front Cell Dev Biol* 9:686907. 10.3389/fcell.2021.686907.

Zhang P, Xu Y, Chen S, Wang Z, Zhao L, Chen C, Kang W, Han R, Qiu J, Wang Q, Gao H, Wu G, and Xia Q. 2022. ARL4C Regulates the Progression of Clear Cell Renal Cell Carcinoma by Affecting the Wnt/beta-Catenin Signaling Pathway. *J Oncol* 2022:2724515. 10.1155/2022/2724515.

Figure 1 Expression and clinical significance of TTC13 in ccRCC. (A) The differential expression of TTC13 between normal and various tumors samples based on the TCGA database; (B) The differential expression of TTC13 between ccRCC and normal tissues (tumor = 539, normal = 72) ($P< 0.001$); (C) Pairing diagram of TTC13 expression in ccRCC and normal tissues (tumor = 72, normal = 72) ($P< 0.001$); (D)TTC13 expression in clinical samples measured by RT-PCR (tumor = 64, normal = 64) ($P< 0.001$); (E) TTC13 expression in clinical samples determined by western blot; (F)TTC13 expression in clinical samples determined by

IHC;(G)TTC13 expression in ccRCC cell lines detected by western blot; (H) The ROC curves of 1, 3 and 5 year survival of ccRCC patients; (I)K–M survival analysis of TTC13 in ccRCC ($P< 0.001$).

Figure 2 TTC13 promoted the proliferation as well as inhibited the apoptosis and autophagy in ccRCC. 786-0 and Caki-1 cells were transfected with pLTTC13, shTTC13 or vector controls. The proliferation of HK-2,786-0 and Caki-1 cells was determined by CCK-8. Three biological replicates were performed in each group (A); The apoptosis and autophagy related protein expression in HK-2, 786-0 and Caki-1 cells was analyzed by flow cytometry (B) and western blot (C), respectively.

Figure 3 TTC13 silencing inhibited tumor growth in vivo. (A) shTTC13 or vector control-transfected 786-0 cells were injected subcutaneously into the nude mice; (B)Tumors from the two groups; (C) Comparison of tumor weight between the two groups; (D)Comparison of tumor volumes between the two groups; (E) IHC staining of the indicated tumor tissues; (F) The expression of indicated proteins were examined by western blot.

Figure 4 TTC13 related signaling pathways in ccRCC. (A) Up- and down-regulated signaling pathways were identified by GSVA analysis;(B) The expression of Wnt/β-catenin signal pathway in 6 paired ccRCC tissues; (C) The expression of IL6-JAK-STAT3 signal pathway in 6 paired ccRCC tissues; (D) TTC13 overexpression enhanced Wnt/β-catenin and IL6-JAK-STAT3 signal pathways, while knockdown of TTC13 displayed the opposite effect.

Figure 5 TTC13 promoted ccRCC growth through Wnt/β-catenin and IL6-JAK-STAT3 signal pathway. AG490: JAK inhibitor; ICG001: WNT inhibitor. (A) Apoptosis of 786-0 and Caki-1cells was detected by flow cytometry. AG490: 20μM; ICG001:10μM ; (C) TTC13 promoted 786-0 and Caki-1 cell proliferation via Wnt/β-catenin and IL6-JAK-STAT3 signal pathways, as determined by CCK-8 assay.AG490 concentration: 50μM; ICG001:20μM. Five biological replicates were performed in each group; (B) Dose response curve. Cells were treated with difference doses of indicated inhibitors for 3 days, and the cell proliferation was measured;(D) TTC13 regulated Wnt/β-catenin and IL6-JAK-STAT3 signal molecule expression was determined by western blot in 786-0 and Caki-1 cells.

Figure 6 STAT3 regulated TTC13 expression at the transcription level. (A, B) Specific binding sites of STAT3 in the promoter region of TTC13 gene;(C) Changes in endogenous TTC13 levels bySTAT3 knockdown or overexpression; (E) CHIP assay verified that STAT3 directly bound to TTC13 promoter;(F)

The luciferase reporter assay confirmed the binding of STAT3 to TTC13 promoter region;(D) Immunofluorescence (IF) staining demonstrated a clear STAT3 nuclear translocation induced by TTC13 overexpression.

Figure7 A working model of TTC13 regulation in ccRCC cells.

Figure 1S TTC13 expression is associated with 8 clinicopathological characteristics including age, gender, race, grade, stage, TNM stage in ccRCC(A-H).

Figure 2S GSEA diagram of TTC13 related signaling pathways. (A) Apoptosis signaling pathway; (B) Transcription factors signal pathway; (C) JAK-STAT signal pathway; (D) Regulation of autophagy signal pathway; (E) Wnt signaling pathway; (F) Renal cell carcinoma signaling.

Figure 3S The associations between TTC13 and immune cell.

Figure 4S TTC13 predicts the immune response and drug sensitivity of ccRCC. (A-E) The associations between TTC13 and TAM M2, CAF, dysfunction, CD274 and TIDE; (F-H) Correlations between TTC13 expression and drug sensitivity. Pazopanib, Sorafenib, and Sunitinib were tested.

Figure 5S TTC13 is an independent prognostic factor of ccRCC and the establishment of a nomogram. (A) Univariate Cox regression analysis of 8 clinicopathological parameters with TTC13 in ccRCC; (B) Multivariate Cox regression analysis of 8 clinicopathological parameters withTTC13 in ccRCC; (C) A nomogram to predict ccRCC patients' survival; (D) Calibration curves for 1-, 3-, and 5-year survival of ccRCC patients.

Figure 6S TTC13 expression before and after mouse tumor xenografts experiments.

Figure 1

Fig1

Expression and clinical significance of TTC13 in ccRCC.

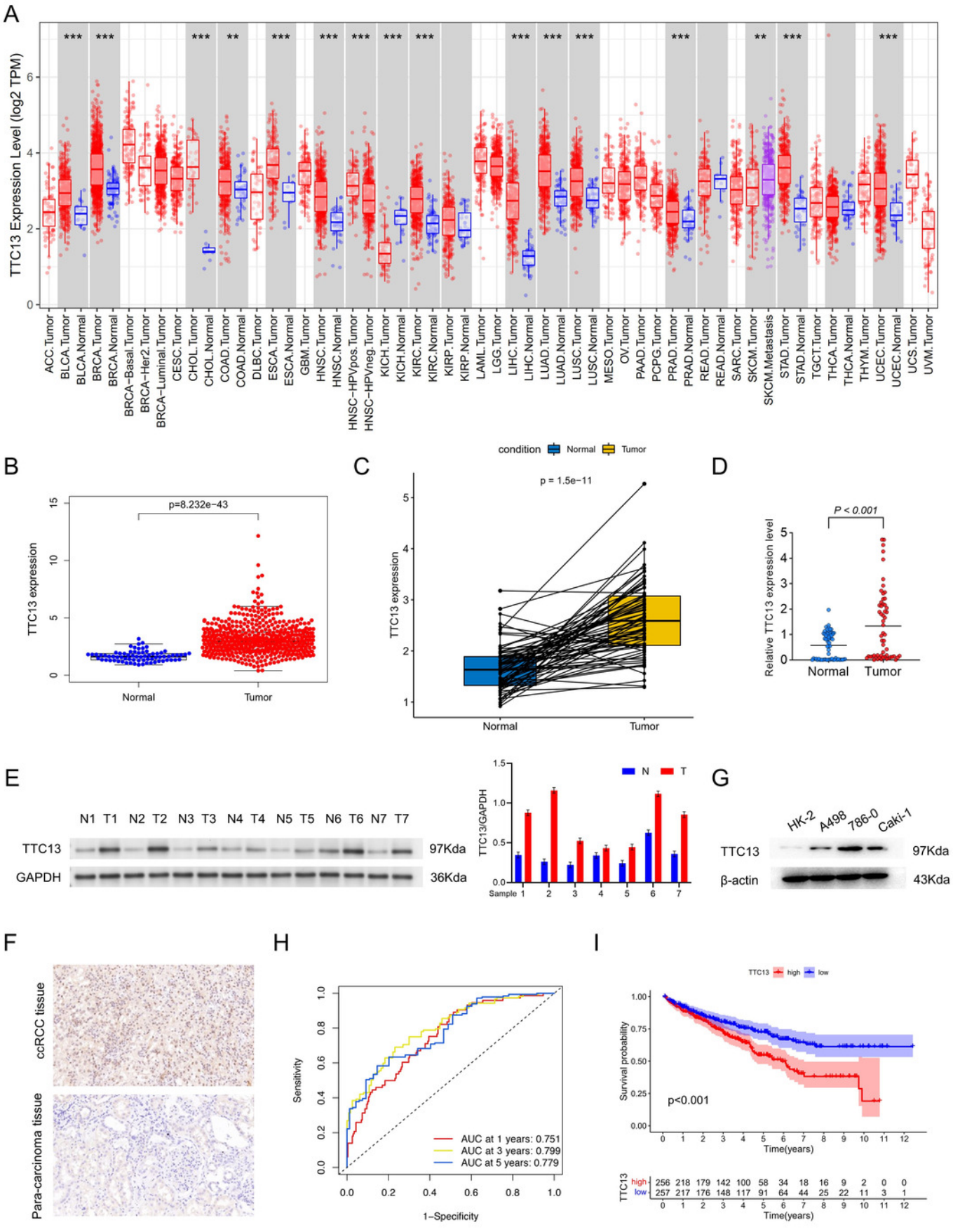
A
TTC13 Expression Level (log2 TPM)
B
p=8.232e-43
TTC13 expression
Normal
Tumor
C
condition Normal Tumor
p = 1.5e-11
TTC13 expression
Normal
Tumor
D
P < 0.001
Relative TTC13 expression level
Normal
Tumor
E
N1 T1 N2 T2 N3 T3 N4 T4 N5 T5 N6 T6 N7 T7
TTC13
GAPDH
97Kda
36Kda
TTC13/GAPDH
N T
Sample 1 2 3 4 5 6 7
G
HK-2 A498 786-0 Caki-1
TTC13
β-actin
97Kda
43Kda
F
ccRCC tissue
Para-carcinoma tissue
H
Sensitivity
1−Specificity
AUC at 1 years: 0.751
AUC at 3 years: 0.799
AUC at 5 years: 0.779
I
TTC13 high low
Survival probability
p<0.001
Time(years)
TTC13
high 256 218 179 142 100 58 34 18 16 9 2 0 0
low 257 217 176 148 117 91 64 44 25 22 11 3 1
Time(years)

Figure 2

Fig2

TTC13 promoted the proliferation as well as inhibited the apoptosis and autophagy.

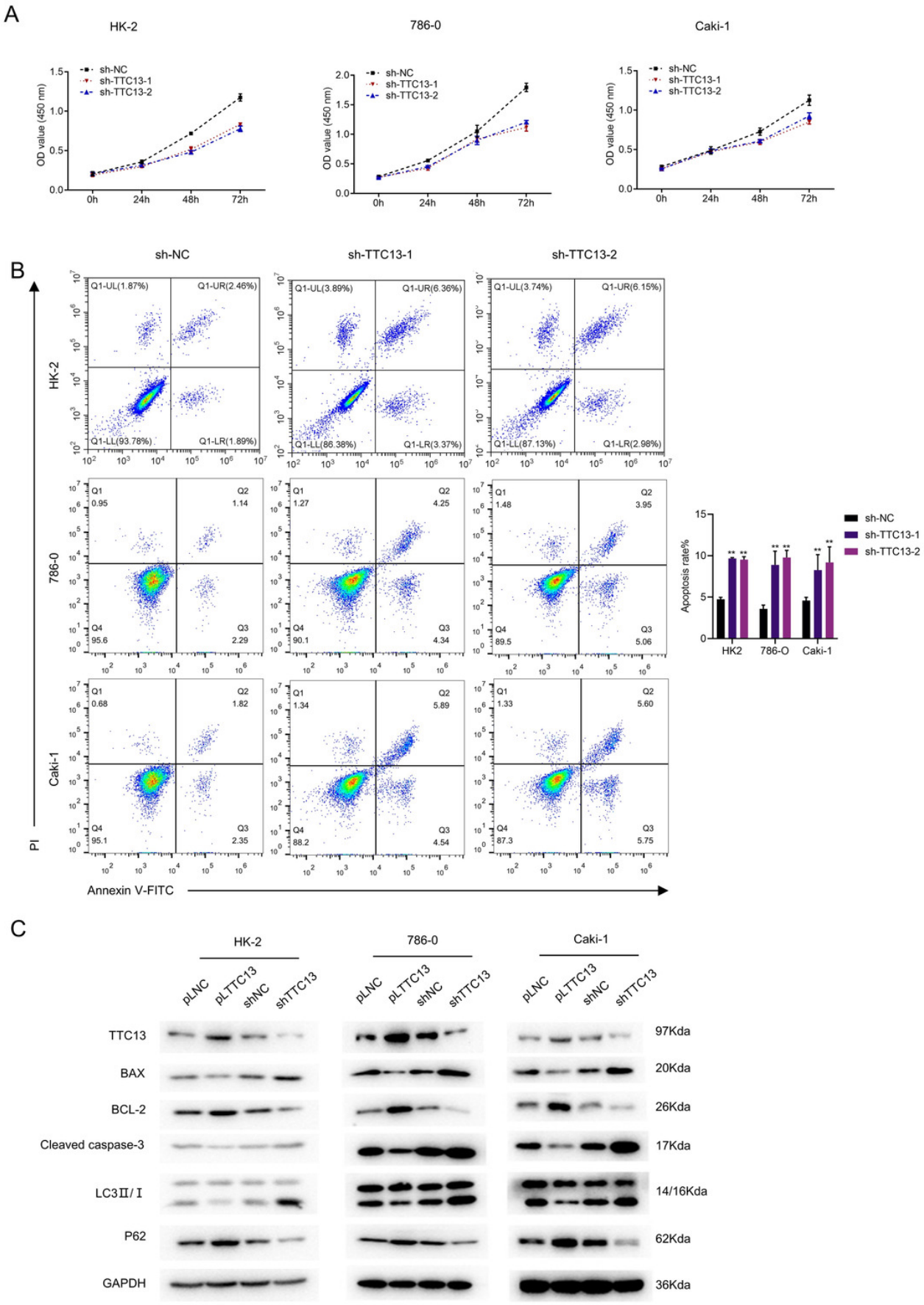
A
HK-2
786-0
Caki-1
sh-NC
sh-TTC13-1
sh-TTC13-2
OD value (450 nm)
0h
24h
48h
72h
B
sh-NC
sh-TTC13-1
sh-TTC13-2
HK-2
786-0
Caki-1
Q1-UL(1.87%)
Q1-UR(2.46%)
Q1-LL(93.78%)
Q1-LR(1.89%)
Q1-UL(3.89%)
Q1-UR(6.36%)
Q1-LL(86.38%)
Q1-LR(3.37%)
Q1-UL(3.74%)
Q1-UR(6.15%)
Q1-LL(87.13%)
Q1-LR(2.98%)
Q1 0.95
Q2 1.14
Q4 95.6
Q3 2.29
Q1 1.27
Q2 4.25
Q4 90.1
Q3 4.34
Q1 1.48
Q2 3.95
Q4 89.5
Q3 5.06
Q1 0.68
Q2 1.82
Q4 95.1
Q3 2.35
Q1 1.34
Q2 5.89
Q4 88.2
Q3 4.54
Q1 1.33
Q2 5.60
Q4 87.3
Q3 5.75
PI
Annexin V-FITC
Apoptosis rate%
HK2
786-O
Caki-1
C
HK-2
786-0
Caki-1
pLNC
pLTTC13
shNC
shTTC13
TTC13
BAX
BCL-2
Cleaved caspase-3
LC3Ⅱ/Ⅰ
P62
GAPDH
97Kda
20Kda
26Kda
17Kda
14/16Kda
62Kda
36Kda

Figure 3

Fig3

TTC13 silencing inhibited tumor growth in vivo.

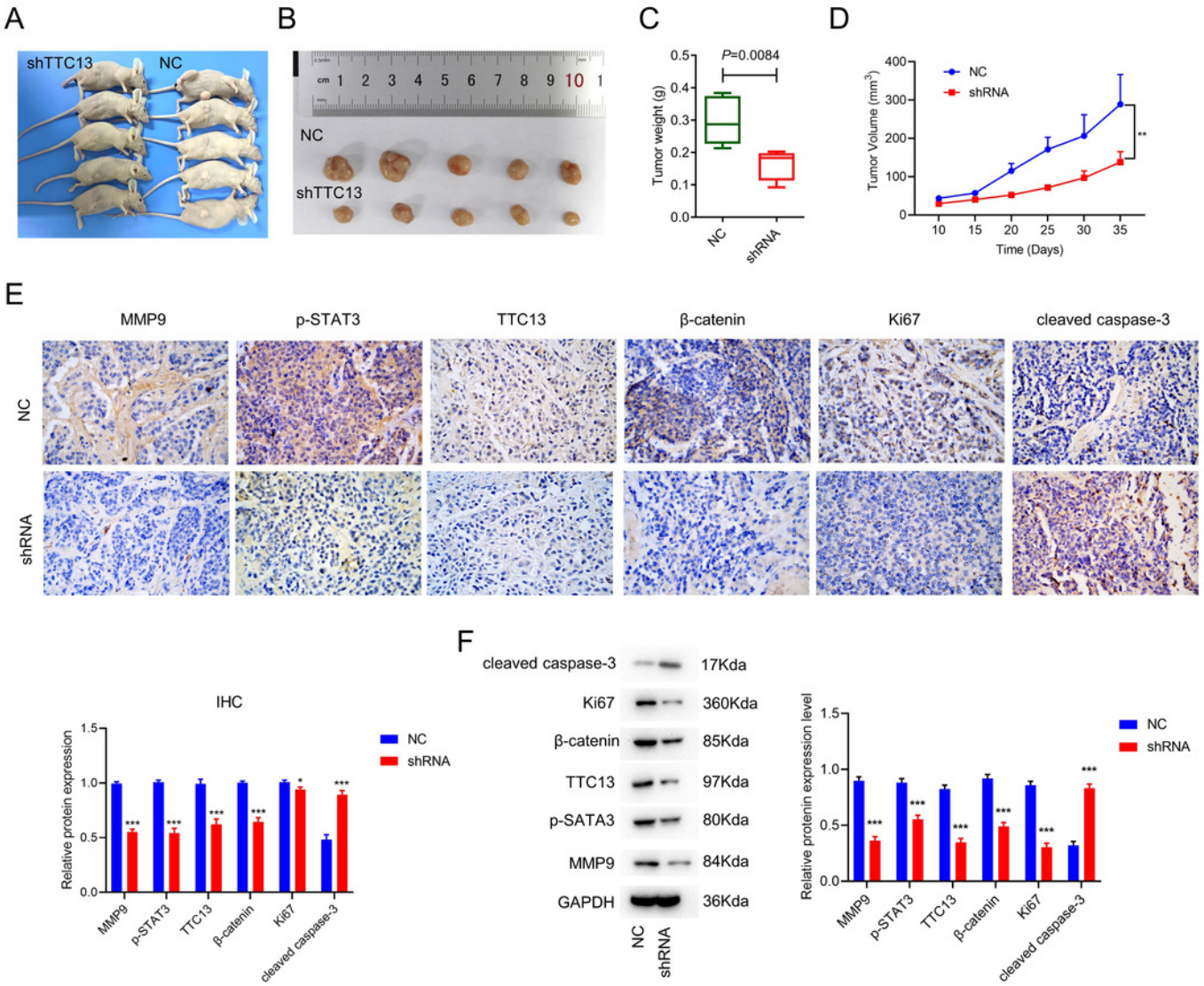

Figure 4

Fig4

TTC13 related signaling pathways in ccRCC.

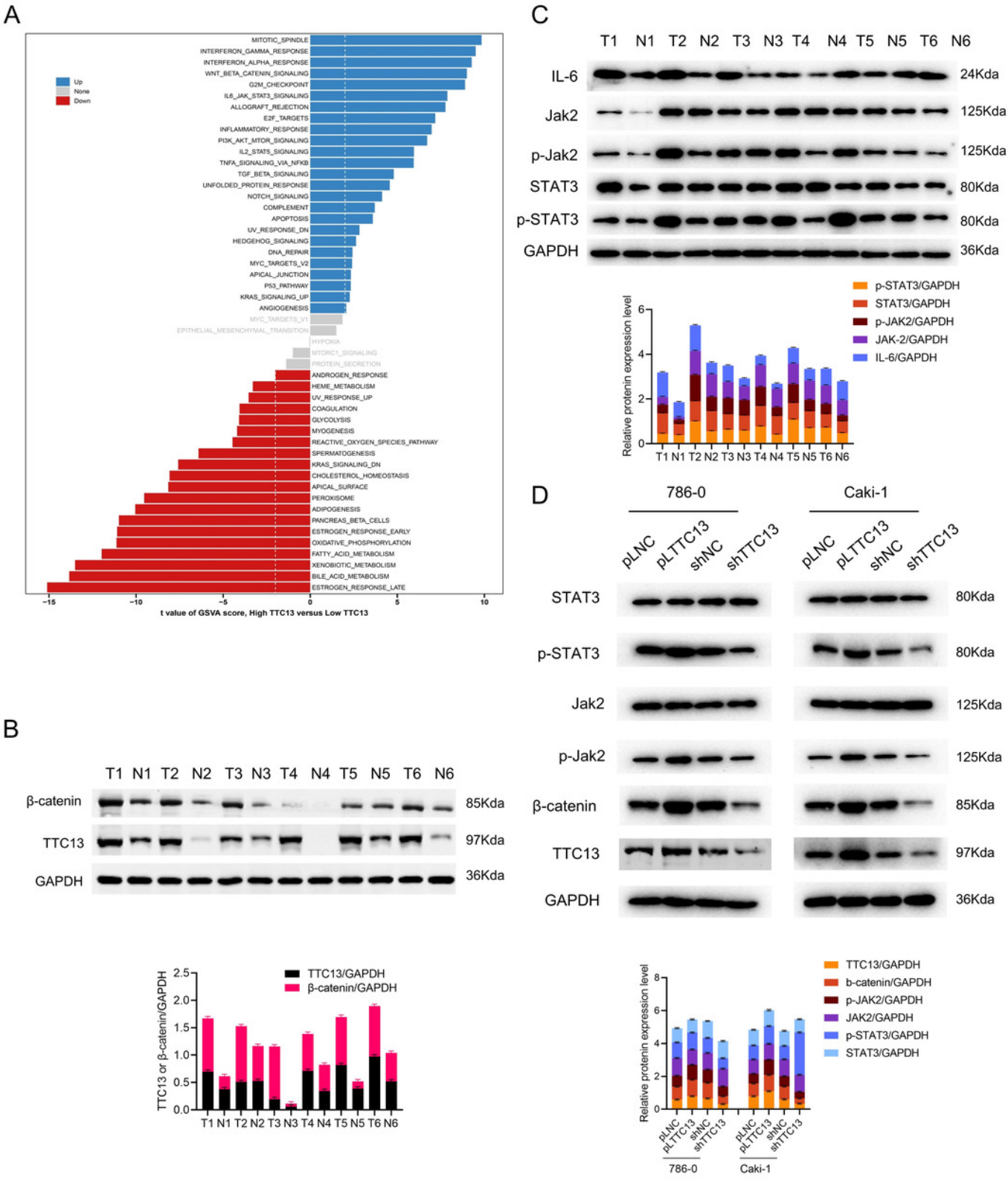
A
MITOTIC_SPINDLE
INTERFERON_GAMMA_RESPONSE
INTERFERON_ALPHA_RESPONSE
WNT_BETA_CATENIN_SIGNALING
G2M_CHECKPOINT
IL6_JAK_STAT3_SIGNALING
ALLOGRAFT_REJECTION
E2F_TARGETS
INFLAMMATORY_RESPONSE
PI3K_AKT_MTOR_SIGNALING
IL2_STAT5_SIGNALING
TNFA_SIGNALING_VIA_NFKB
TGF_BETA_SIGNALING
UNFOLDED_PROTEIN_RESPONSE
NOTCH_SIGNALING
COMPLEMENT
APOPTOSIS
UV_RESPONSE_DN
HEDGEHOG_SIGNALING
DNA_REPAIR
MYC_TARGETS_V2
APICAL_JUNCTION
P53_PATHWAY
KRAS_SIGNALING_UP
ANGIOGENESIS
MYC_TARGETS_V1
EPITHELIAL_MESENCHYMAL_TRANSITION
HYPOXIA
MTORC1_SIGNALING
PROTEIN_SECRETION
ANDROGEN_RESPONSE
HEME_METABOLISM
UV_RESPONSE_UP
COAGULATION
GLYCOLYSIS
MYOGENESIS
REACTIVE_OXYGEN_SPECIES_PATHWAY
SPERMATOGENESIS
KRAS_SIGNALING_DN
CHOLESTEROL_HOMEOSTASIS
APICAL_SURFACE
PEROXISOME
ADIPOGENESIS
PANCREAS_BETA_CELLS
ESTROGEN_RESPONSE_EARLY
OXIDATIVE_PHOSPHORYLATION
FATTY_ACID_METABOLISM
XENOBIOTIC_METABOLISM
BILE_ACID_METABOLISM
ESTROGEN_RESPONSE_LATE
Up
None
Down
t value of GSVA score, High TTC13 versus Low TTC13
B
T1 N1 T2 N2 T3 N3 T4 N4 T5 N5 T6 N6
β-catenin
TTC13
GAPDH
85Kda
97Kda
36Kda
TTC13/GAPDH
β-catenin/GAPDH
TTC13 or β-catenin/GAPDH
C
T1 N1 T2 N2 T3 N3 T4 N4 T5 N5 T6 N6
IL-6
Jak2
p-Jak2
STAT3
p-STAT3
GAPDH
24Kda
125Kda
125Kda
80Kda
80Kda
36Kda
p-STAT3/GAPDH
STAT3/GAPDH
p-JAK2/GAPDH
JAK-2/GAPDH
IL-6/GAPDH
Relative protenin expression level
D
786-0
Caki-1
pLNC
pLTTC13
shNC
shTTC13
STAT3
p-STAT3
Jak2
p-Jak2
β-catenin
TTC13
GAPDH
80Kda
80Kda
125Kda
125Kda
85Kda
97Kda
36Kda
TTC13/GAPDH
b-catenin/GAPDH
p-JAK2/GAPDH
JAK2/GAPDH
p-STAT3/GAPDH
STAT3/GAPDH
Relative protenin expression level

Figure 5

Fig5

TTC13 promoted ccRCC growth through Wnt/β-catenin and IL6-JAK-STAT3 signal pathway.

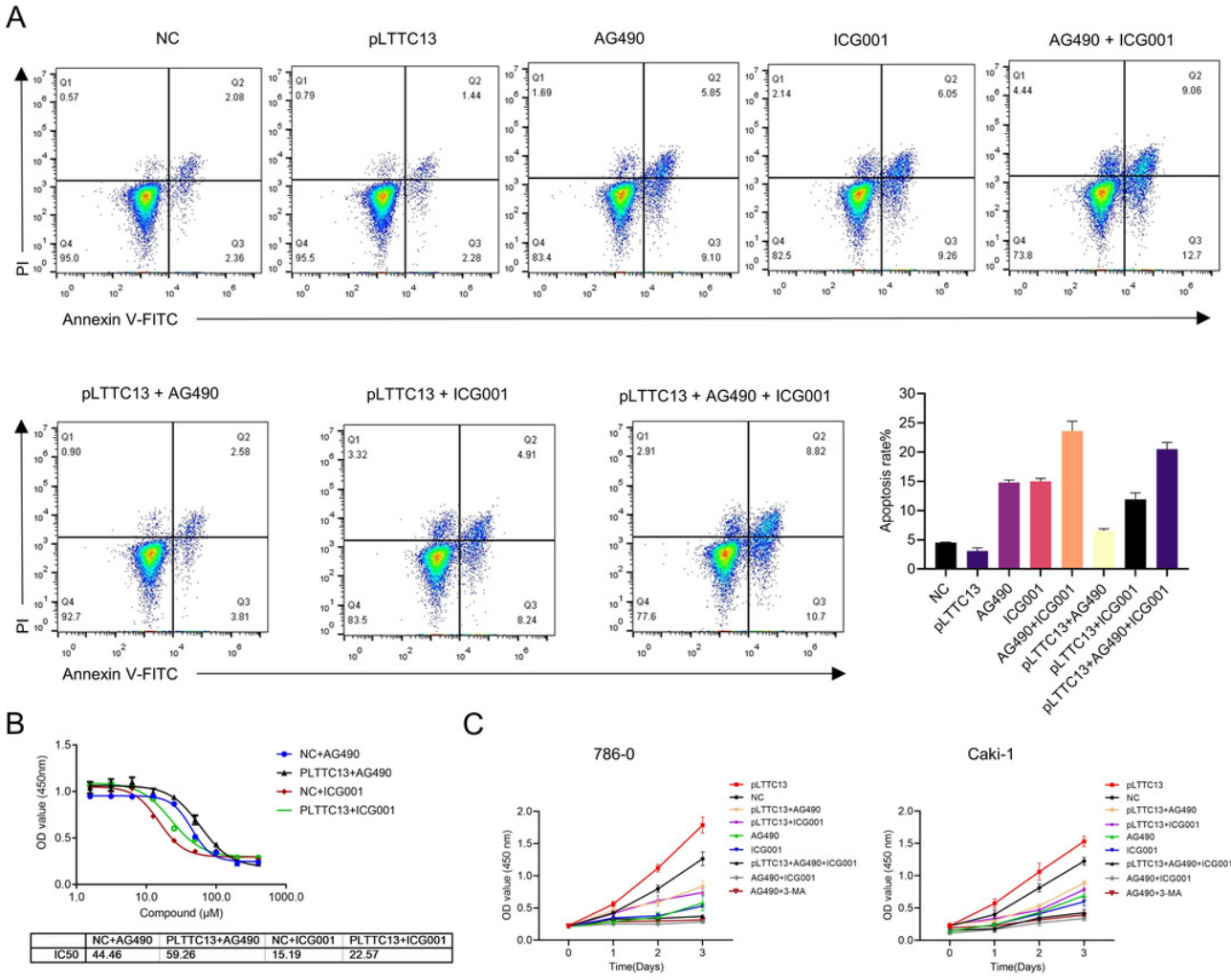

	NC+AG490	PLTTC13+AG490	NC+ICG001	PLTTC13+ICG001
IC50	44.46	59.26	15.19	22.57

Figure 6

Fig6

STAT3 regulated TTC13 expression at the transcription level.

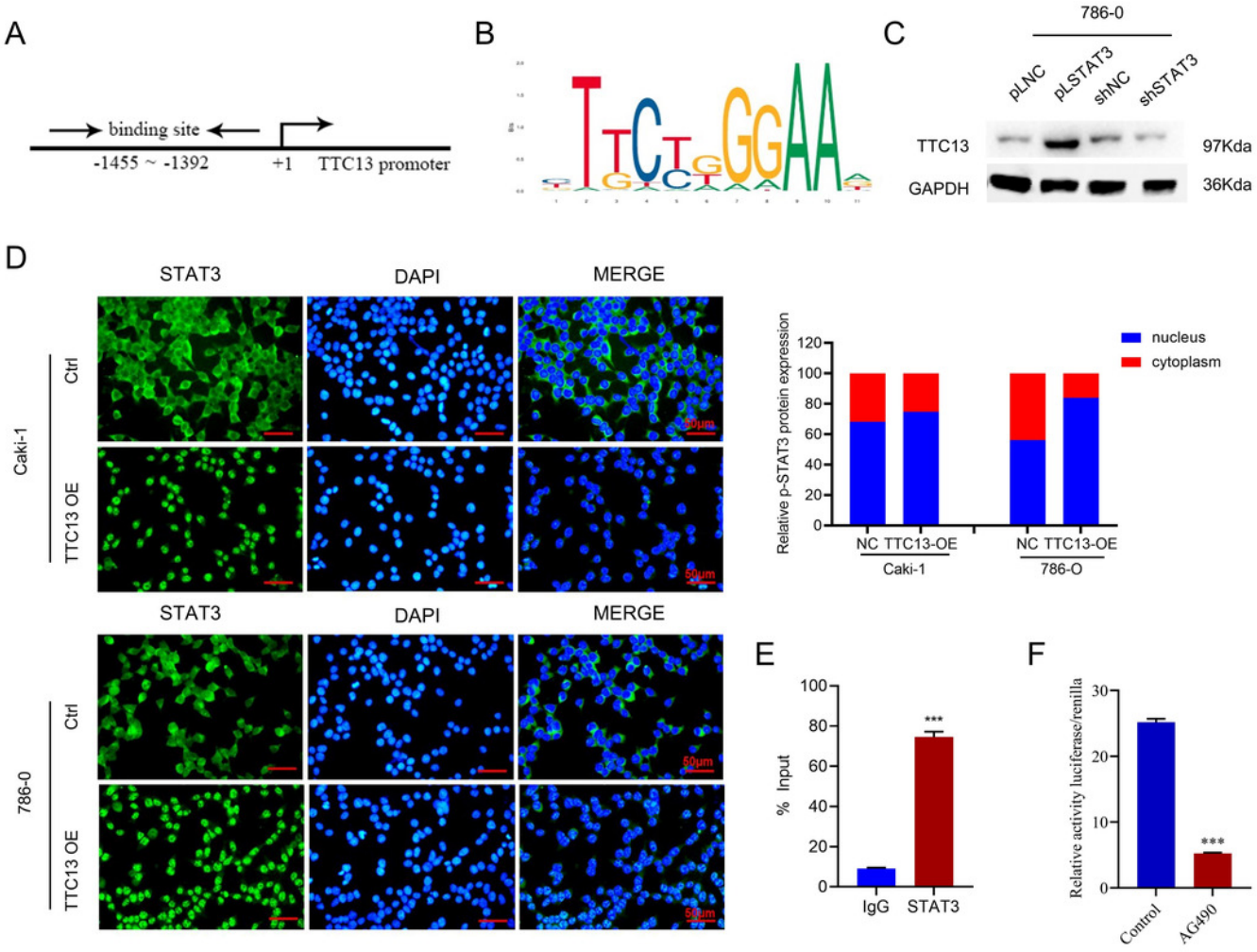

Figure 7

Fig7

A working model of TTC13 regulation in ccRCC cells.